AIAA 2001–0729

Turbulence models in pulsating flows

Alberto Scotti
University of North Carolina, Chapel Hill, NC 27599, USA

and

Ugo Piomelli
University of Maryland, College Park, MD 20742, USA

39th AIAA Aerospace Sciences Meeting and Exhibit
January 8–11, 2001/Reno, NV

Turbulence models in pulsating flows

Alberto Scotti *
University of North Carolina, Chapel Hill, NC 27599, USA

and

Ugo Piomelli †
University of Maryland, College Park, MD 20742, USA

This paper compares the performance of three low-Reynolds-number models for the unsteady Reynolds-averaged Navier-Stokes equations applied to the flow in a channel driven by a pressure gradient oscillating around a non-zero mean. The models considered are the one-equation Spalart-Allmaras model, the $k-\varepsilon$ model with the wall functions of Lam and Bremhorst and the $k-\varepsilon-v^2$ model of Durbin. The results are compared with experiments, direct simulations and large-eddy simulations. The models give similar and reasonably accurate results as far as predicting the velocity profile in the channel as a function of the phase, and reproduce the observed behavior during part of the cycle. However, large differences exist between the models themselves, as well as with respect to the LES, at the level of Reynolds stress, turbulent kinetic energy and dissipation rate. The $k-\varepsilon-v^2$ is overall superior to $k-\varepsilon$ and to the Spalart-Allmaras model.

Introduction

MANY turbulent flows, both natural (the gravity-wave induced bottom boundary layer, the blood flow in large arteries, the flow around swimming fish, *etc.*) and artificial (flows in internal combustion engines, heat exchangers, and so on) are inherently unsteady. The unsteadiness can be due to fluctuations in the driving force, to unsteadiness in the boundary conditions, or to a combination of both. The imposition of external unsteadiness can significantly alter a flow, even resulting in partial or full re-laminarization of an initially turbulent flow. Despite their importance to a variety of fields, and the complexity of the modifications that result from the unsteadiness, flows of this kind have received relatively little attention compared to steady ones. Although models for the unsteady Reynolds-Averaged Navier-Stokes (URANS) equations are routinely used in engineering calculations, their accuracy, especially in view of the alterations of the turbulence physics that may take place in these flows, has not been carefully established

In this paper we will compare the performance of three low-Reynolds-number URANS models applied to the flow in a channel driven by a pressure gradient oscillating around a non-zero mean. The simplicity of the geometry makes it possible to performed direct simulations and well-resolved large-eddy simulations that can be used to validate the URANS models. Furthermore, an analytical solution exists for laminar flow (a simple extension of Stokes' second problem[1]), and experimental data are available.[2–4]

The flow is controlled by three parameters. The mean pressure gradient ensures that the turbulent quantities oscillate around a non-zero mean. The mean wall stress can be used to define a mean friction velocity u_τ that, in conjunction with the viscosity ν, defines wall units. A second parameter is the forcing frequency $\omega^+ = \omega\nu/u_\tau^2$, or alternatively the Stokes length $l_s^+ \equiv (2/\omega^+)^{1/2}$, a measure of how far the vorticity waves generated by the unsteady pressure gradient penetrate the laminar flow. The ratio between oscillating and steady centerline velocity a_{uc} completes the parameter space; when $a_{uc} < 1$ (current-dominated flow), experiments show that the flow is largely controlled by ω^+; we will concentrate on this case, which is prevalent in the ocean.[5]

The experimental evidence[2–4] shows that at very low frequencies the turbulence has time to relax to the local (in time) equilibrium. As the frequency is increased, however, typical turbulent quantities such as the ratio $\langle u'u'\rangle/\langle q^2\rangle$ begin to exhibit a phase dependence, which might indicate that production and dissipation are out of phase. In this regime the flow can transition from a fully turbulent state to a quasi-laminar one within a wave cycle. At very high frequencies the flow can be assumed to be the superposition of a steady part plus the laminar Stokes solution for the given frequency. In this regime, the unsteadiness is confined within the viscous sublayer, while the turbulence in the outer layer is frozen and oscillates as a plug flow. The effects of the steady flow on the oscillating part are more subtle. The most notable (and counter-intuitive) one is the fact that, for $0.02 < \omega^+ < 0.06$,

*Department of Marine Sciences
†Department of Mechanical Engineering. AIAA Senior Member.

the amplitude of the oscillation of the wall stress is *lower* than the value it would have were the flow to be purely laminar. In other words the background turbulence may reduce the shear.

Despite its simplicity, this flow is an extremely challenging test-case for unsteady RANS models. The fact that turbulence is out of equilibrium, and that the re-laminarization and re-transition may take paths dependent on the frequency constitute a severe challenge for conventional RANS models. However, most of the models used in the literature are extensions of steady eddy-viscosity closures, with different recipes to compute the eddy viscosity.[6,7] One notable exception is the model proposed by Mankbadi and Liu,[8] which is based on rapid distortion theory and it is a true unsteady model. The model of Mankbadi and Liu[8] captures some of the features when the frequency approaches the quasi-steady limit, but fails to reproduce the regime at higher frequencies. Mao and Hanratty[9] have proposed a model that reproduces qualitatively the turbulent-induced reduction in amplitude described above, based on the premise that the main effect of the oscillating pressure gradient is to change the height of the viscous layer. A relaxation relation is used to compute this height, which is hence out of phase with the outer layer. The eddy viscosity is computed using Reichardt's[10] formula for the core region, while for the near-wall the mixing length approach with van Driest damping[11] is used. The damping length is assumed to be proportional to the height of the wall layer. By the authors' own admission, the model has very little physical justification, and, furthermore, depends on constants that have to be fine-tuned. Nonetheless, it points to the fact that the heaving of the wall layer plays an important role.

To calculate accurately flows of this type using engineering techniques, a better understanding of the capabilities and limitations of URANS models is required. Direct and large-eddy simulation data can be very useful in helping to achieve this goal. Thus, in this paper we will test three well-established URANS models using data from large-eddy simulations (LES) and direct simulations (DNS) as reference. In the following, after briefly reviewing the numerical dataset used as benchmark we will describe the models used. Then, the models will be evaluated *a priori* (using the data from the LES, experiments and DNS to compute the Reynolds stresses according to the prescription of the model) and *a posteriori* (comparing the URANS results with LES and DNS). At the end, some conclusions will be drawn.

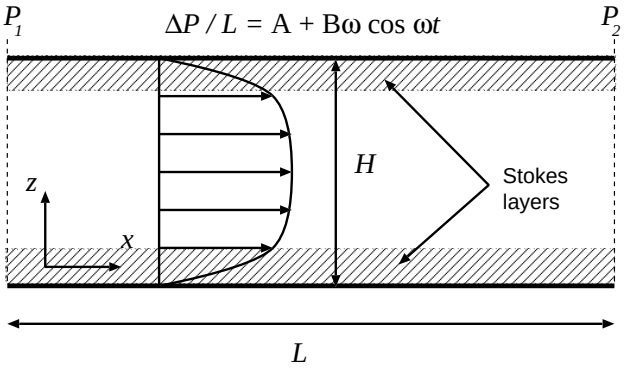

Fig. 1 Sketch of the channel geometry.

Problem formulation and numerical datasets

We have simulated the flow in a channel with periodic boundary conditions in the spanwise and streamwise directions. The geometry is sketched in Fig. 1. The flow is forced by a pressure gradient given by

$$P_f(x,t) = \Delta P_o[1 + \alpha\cos(\omega\, t + \pi/2)]x/L_x, \quad (1)$$

so that the flow begins the acceleration phase at $t/T = 0$. By setting $\Delta P_o/L_x = 1.0 \times 10^{-4}$, the Reynolds number based on the mean friction velocity $u_\tau = \sqrt{H\Delta P_o/2\rho L_x}$ and channel half-height is equal to 350, while the one based on the mean centerline velocity is approximatively equal to 7200. In all calculations a_{uc} was close to 0.7. The frequency was varied from 0.02 to 0.0008. Table 1 lists the relevant parameters.

The reference data was obtained from DNS and LES of this flow that were performed using a well-established spectral code.[12] The DNS used $128\times129\times192$ point in the streamwise, wall-normal and spanwise directions to discretize a domain whose size was $3\pi H \times H \times \pi H$ (H is the channel height). The LES used $64\times65\times64$ points to discretize the same domain, and the subgrid-scale stresses were modeled using the dynamic eddy-viscosity model.[13,14] The LES were validated by comparison with the DNS at high frequency, and with experiments at intermediate and low frequencies, and found to be in good agreement with the existing data. Detailed comparisons between the LES, DNS and experiments are presented in a forthcoming article.[15]

Description of the URANS models

Due to the simple geometry, the URANS equation for the horizontal momentum simply becomes

$$\frac{\partial U}{\partial t} = -\frac{\partial P_f}{\partial x} + \frac{\partial}{\partial y}\left(\nu\frac{\partial U}{\partial y} - \langle u'v'\rangle\right), \quad (2)$$

	High Frequency	Medium Frequencies	Low Frequency
ω	0.02	0.005–0.0022	0.0008
l_s^+	7	14–21	35

Table 1 Simulation parameters.

where $\langle\cdot\rangle$ denotes phase-averaging, and $U = \langle u_1 \rangle$. We have selected three commonly used URANS model for this study. In order of increasing computational complexity they are the one-equation model of Spalart and Allmaras,[16] a standard $k-\varepsilon$ model with the wall correction of Lam and Bremhorst[17,18] and the $k-\varepsilon-v^2$ model of Durbin.[19] All models assume the existence of an eddy viscosity that is used to express the Reynolds stress as

$$-\langle u'v' \rangle = \nu_t \frac{\partial U}{\partial y}. \tag{3}$$

Below we briefly review each model and we indicate the parameters used. All the models were run first with a steady pressure gradient, and the results compared with the DNS data of Moser *et al.*[20] for channel flow at $Re_\tau = 395$ (the DNS data was also used to provide the initial condition).

Spalart-Allmaras one-equation model

The Spalart-Allmaras[16] one-equation model (in the following referred to as SA) is gaining increased popularity for the calculation of aerodynamic flows, both in the contest of steady or unsteady RANS calculations, and in the approach known as "Detached Eddy Simulation".[21] In this model a non-linear transport equation is solved for the eddy viscosity. This equation includes the effects of production, diffusion, wall blocking, destruction and finite-Reynolds number near the wall. All terms in the equation are developed based on phenomenological considerations.

$k-\varepsilon$ two-equation model

The $k-\varepsilon$ model may be the most commonly used model in engineering applications. The eddy viscosity is given by

$$\nu_t = C_\mu \frac{\langle k \rangle^2}{\langle \varepsilon \rangle}, \tag{4}$$

where $\langle k \rangle$ is the phase-averaged turbulent kinetic energy and $\langle \varepsilon \rangle$ the phase-averaged rate of dissipation. Transport equations for the turbulent kinetic energy k and the dissipation ε are then solved. Many formulation of this model exist, and especially the near-wall treatments may differ significantly. Our choice of the model proposed by Lam and Bremhorst[17] was motivated by the fact that this formulation does not require the use of the instantaneous u_τ. In the configuration under study, the flow may reverse its direction, and the phase-averaged wall stress may vanish. This feature makes any model that requires the use of wall variable liable to fail. We refer to this model as KE.

$k-\varepsilon-v^2$ model

The $k-\varepsilon-v^2$ (referred to as KEV2) model proposed by Durbin[19] represents an extension of the standard $k-\varepsilon$ model. The eddy viscosity is taken to be

$$\nu_t = C_\mu \frac{\langle v^2 \rangle \langle k \rangle}{\langle \varepsilon \rangle} \tag{5}$$

where $\langle v^2 \rangle^{1/2}$ is a velocity scale (in this geometry $\langle v^2 \rangle$ represents the intensity of vertical fluctuations). To include the effects of the pressure-strain term (which is absent in the equation for k), an auxiliary equation is introduced that accounts for the blocking effect of the wall. We have calibrated the model using the DNS data at $Re_\tau = 395$,[20] resulting in slightly different values for some of the coefficients, compared to their standard ones. The values used are shown in Table 2 below.

Numerical aspects

All models were solved using the same numerical scheme. The spatial discretization was performed using second-order finite differences on a non-uniform grid (stretched to accommodate 10 points within $y^+ < 10$). The derivatives of $\langle v^2 \rangle$ in the KEV2 model, however, were computed using a fourth-order scheme, since $\langle v^2 \rangle \sim y^{+4}$ near the wall, so that a second-order scheme would produce errors of the the same order as the derivative itself. A third-order Runge-Kutta scheme was used to advance the non linear part of the equations, while the linear part was treated implicitly with a Crank-Nicholson scheme. The initial conditions were obtained from the LES data. The model was run for a total of 10 wave cycles to remove initial transients.

Physical description of the flow

Details of the flow can be found elsewhere.[2–4,15] For the sake of completeness, however, we summarize briefly the main points observed by previous researchers.

The unsteady pressure gradient at the wall generates waves of vorticity that propagate away from the wall, while being attenuated. The penetration length in turbulent flow, l_t^+, is proportional to l_s^+ at high frequencies; at low frequencies, however, l_t^+ scales as l_s^{+2}. Only if l_t^+ is large enough inner and outer layer are significantly coupled; in our calculations that was the case at intermediate and low frequencies. At high frequencies, on the other hand, the turbulence in the outer zone is convected by the oscillating flow as a plug flow.

The centerline velocity, shown in Fig. 2, lags behind the stress at the wall; the phase difference is $\pi/4$ at high frequencies, and drops to zero at low frequencies, where the flow is essentially in equilibrium.[22] The good agreement between DNS and LES at the high frequency can also be observed in this figure. At high

	C_μ	C_{ε_2}	C_1	C_2	C_L	C_η
Original	0.19	1.9	1.4	0.3	0.3	70.
Modified	0.21	1.9	1.22	0.4	0.2	80.

Table 2 Original and modified parameters in the $k-\varepsilon-v^2$ model.

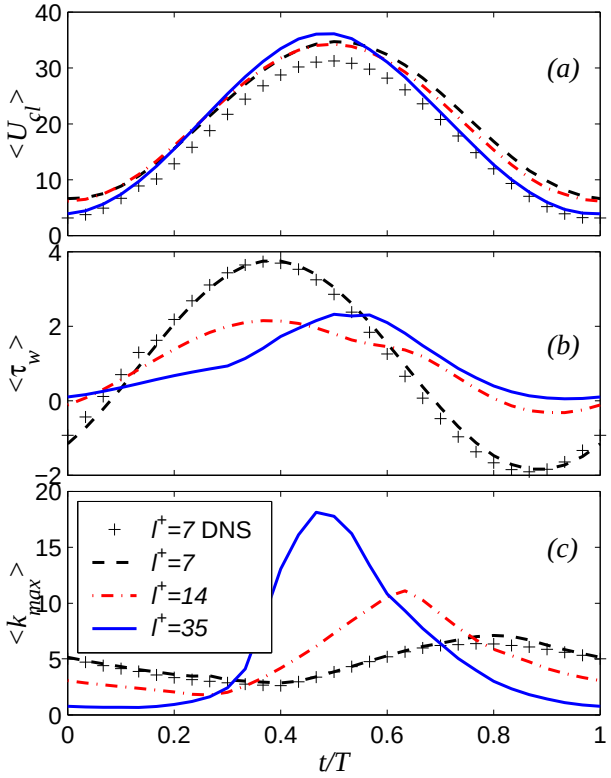

Fig. 2 Time series of the (a) centerline velocity; (b) wall stress; (c) maximum of the turbulent kinetic energy k.

frequencies the response of the system is essentially at the driving frequency, despite the non-linear character of the equations. As the frequency is lowered, however, higher harmonics are excited.

It is interesting to note the asymmetric response of the turbulent kinetic energy at low and intermediate frequencies: at the lowest frequencies the flow at the beginning of the acceleration phase is essentially laminar (although the velocity profile is not, as the viscous time needed to relax to the Poiseuille profile $t^+ \sim Re_\tau^2$ exceeds the period). Figure 3 shows contours of the streamwise velocity fluctuations u' during the cycle. One can observe a nearly quiescent flow for $t/T = 0$. As the flow picks up momentum, very long and smooth streaks develop, which, eventually, become unstable and burst into a localized turbulent spot, at $t = 3T/8$, which eventually fills the whole channel. At high frequencies, the process is very different (Fig. 4). Fairly healthy streaky structures can be observed for the entire period. During the acceleration phase the flow begins to re-laminarize: some very long, nearly straight low-speed streaks can be observed ($1/8 \leq t/T \leq 2/8$).

A priori testing

A first evaluation of the model accuracy can be performed *a priori* by computing the Reynolds stresses and the eddy viscosity using the "true" velocity field, represented here by the LES data. This comparison allows us to evaluate the validity of the modeling *ansatz per se*, removing possible errors that may be due to the modeling of the terms in the k or ε equations. Accordingly, we have computed the Reynolds stresses from (3) using the LES data for U, k, ε and $\overline{v}^2$ in (4–5).

The peak Reynols shear stress is shown in Fig. 5 for the KE and KEV2 models. KEV2 is able to reproduce the maximum value of the phase-averaged Reynolds shear stress fairly well, although at low frequencies it tends to overestimate the stress growth during the acceleration phase. The performance of KE is poorer: the peak Reynolds shear stress is very significanly overstimated during the acceleration phase.

Significant differences between the two models can be observed in the shapes of the profiles as well, which are shown in Fig. 6, normalized by their maximum value. KEV2 is able to reproduce the shape of the Reynolds stress fairly well, the most notable exception being a tendency during the acceleration phase to overestimate the stress growth in the inner region. With the KE model, on the other hand, not only is the peak stress in the inner region much larger than observed in the LES, but also the relative stress in the outer region is often too small. While the former fact could be ameliorated by a different choice of wall functions, the latter result should be viewed as an intrinsic shortcoming of the of the k^2/ε ratio. The acceleration phase, in fact, is accompanied by a decrease in the structure parameter

$$a_1 = -\frac{\langle u'v' \rangle}{2k}, \tag{6}$$

which indicates that turbulence is less efficient in extracting shear from the available energy.[15] This decrease is characteristic of the response of many turbulent flows when they are perturbed from equilibrium. In this flow, it is also accompanied by a decrease of the dissipation ε during the relaminarization that takes place during the acceleration; thus, the eddy viscosity predicted by the KE model increases (the denominator decreases, while the numerator decreases less rapidly than the shear stress), while the actual Reynolds stress decreases.

A posteriori testing

We now compare *a* posteriori the predictions of the URANS models with the experimental results collected by Tardu and coworkers,[2–4] as well as with the LES data. Figure 7 shows the phase-averaged velocity streamwise profiles at intervals of $T/4$. All the model predictions are in reasonable agreement with the LES data. Assuming that the effect of turbulence can be captured, at least qualitatively, by a simple eddy viscosity ν_t, and drawing an analogy to the laminar Stokes problem, the effect of the oscillation on the

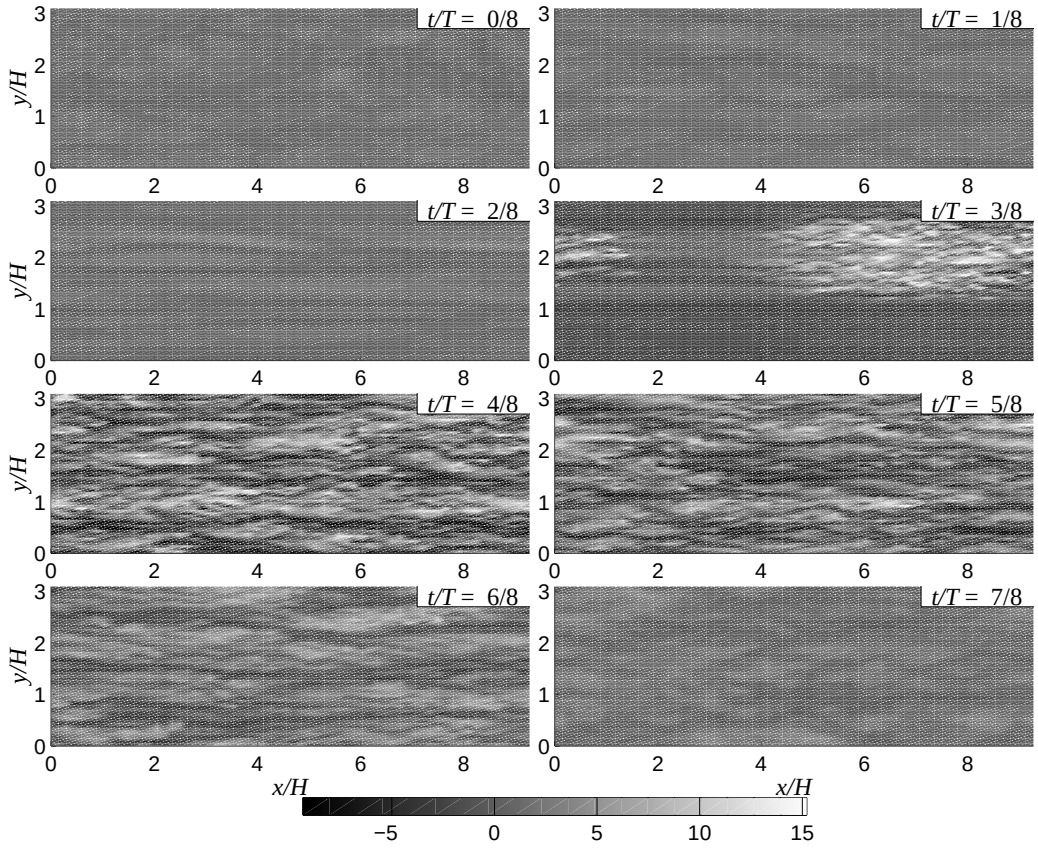

Fig. 3 Contours of the streamwise velocity fluctuations in the $z^+ = 10$ plane. $l_s^+ = 35$.

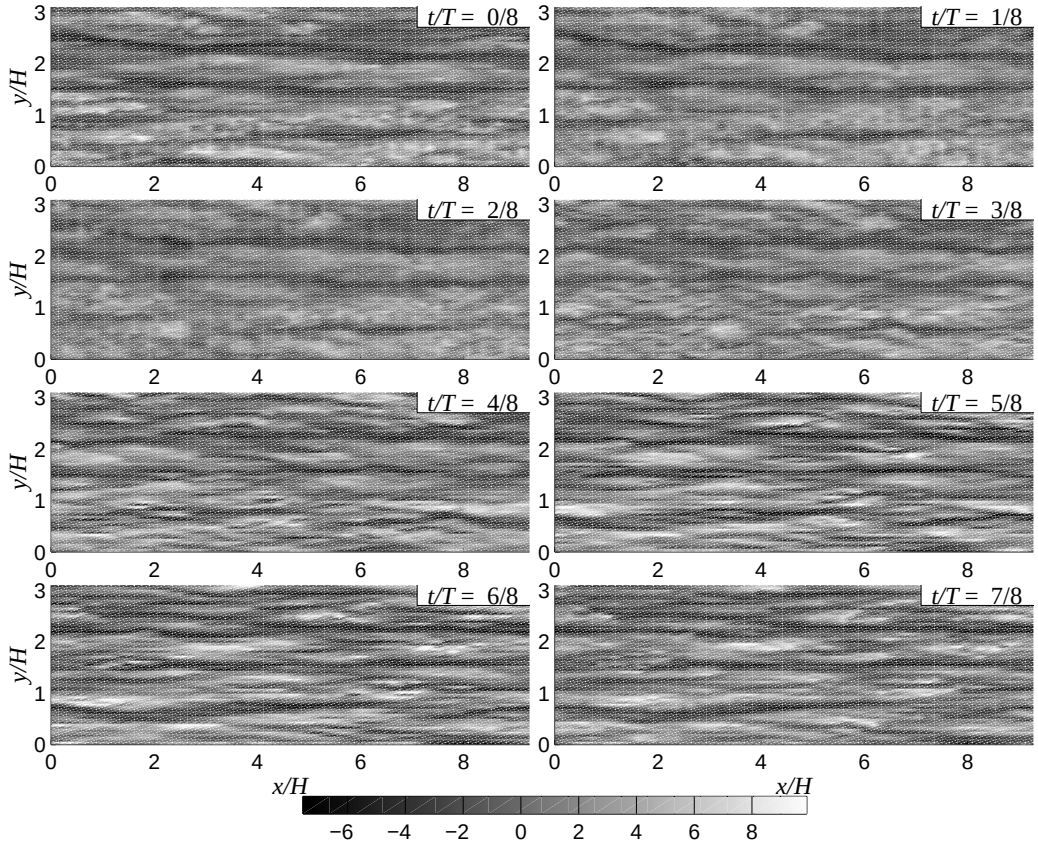

Fig. 4 Contours of the streamwise velocity fluctuations in the $z^+ = 10$ plane. $l_s^+ = 7$.

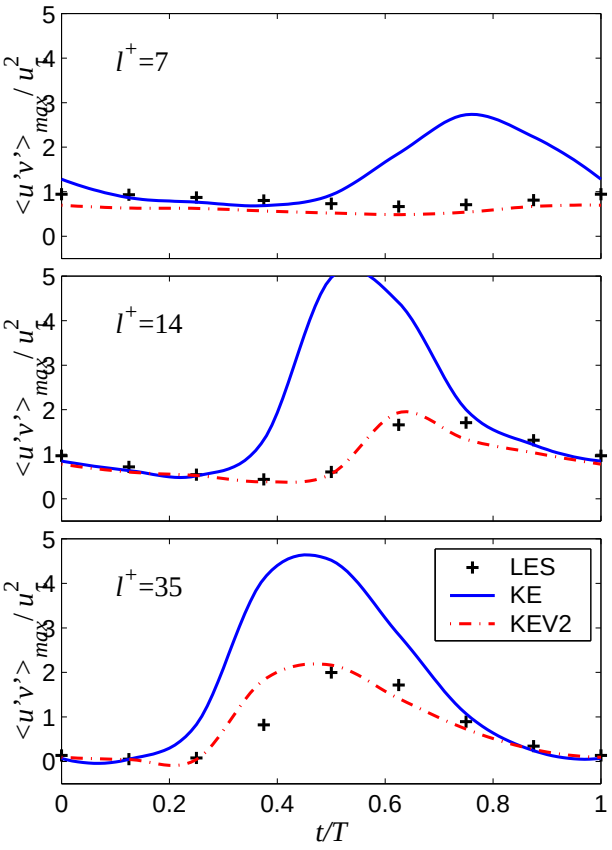

Fig. 5 Time series of the maximum phase-averaged Reynolds shear stress $\langle u'v' \rangle$.

flow should be confined to a layer of thickness of order l_t, where

$$l_t = [2(\nu + \nu_t)/\omega]^{1/2} \tag{7}$$

is a turbulent Stokes length obtained using the sum of the molecular and turbulent diffusivities. Taking for the eddy viscosity $\nu_t = \kappa u_\tau l_t$, where κ is the von Kármán constant, it follows that

$$l_t^+ = l_s^+ \left[\left(\frac{\kappa l_s^+}{2} \right) + \sqrt{1 + \left(\frac{\kappa l_s^+}{2} \right)^2} \right]. \tag{8}$$

The agreement between models and LES is generally better for $y+ > l_t^+$, *i.e.*, outside the layer affected by the unsteadiness. At high frequency KE and KEV2 are very close to each other and essentially match the LES. SA departs from the LES profile more consistently, especially at the end of the deceleration phase (top profile). At intermediate frequencies the discrepancy between URANS models and LES is more evident, especially during the deceleration phase.

A significant contribution to the differences between the models and the LES is due to the error in the prediction of the time-averaged velocity,

$$u_0^+ = \frac{1}{T} \int_0^T \langle u+ \rangle dt, \tag{9}$$

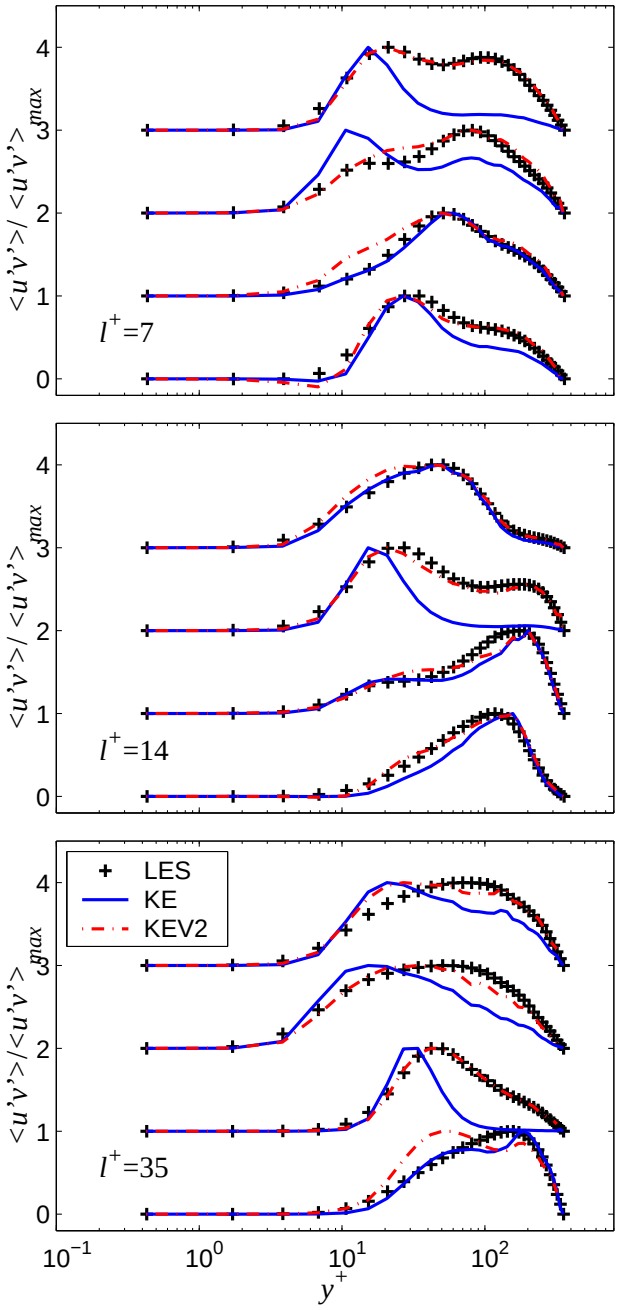

Fig. 6 *A priori* **evaluation of the Reynolds stress $\langle uv \rangle$ using LES data. Profiles are plotted every $T/4$ and offset in the vertical direction; the bottom plot corresponds to $t/T = 0$.**

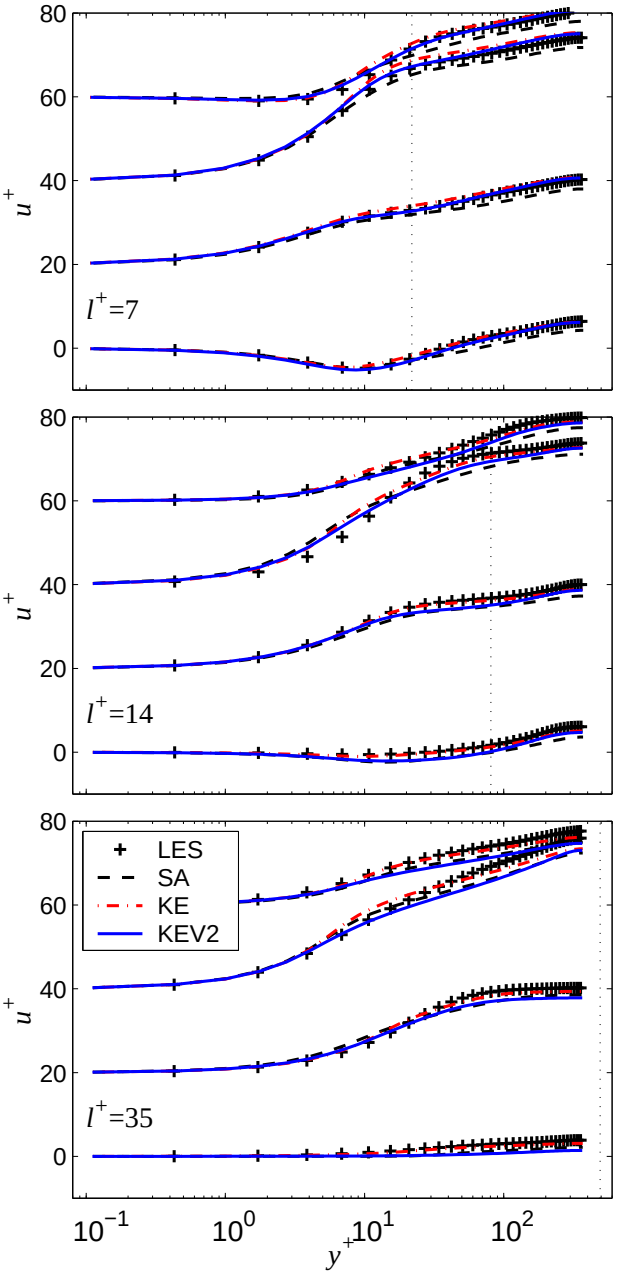

Fig. 7 Profiles of the phase-averaged streamwise velocity. Profiles are plotted every $T/4$ and offset in the vertical direction; the bottom plot corresponds to $t/T = 0$. The dotted line corresponds to the turbulent penetration length l_t^+ given by (8).

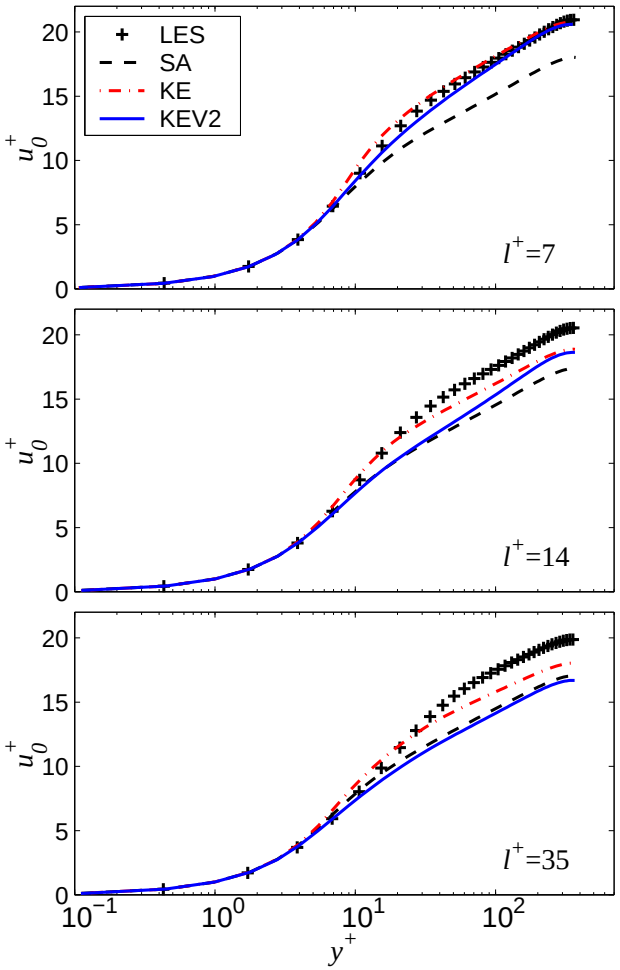

Fig. 8 Time-averaged streamwise velocity.

which is shown in Fig. 8. All models under-predict the ratio u_τ/U_b (where U_b is the average velocity in the channel) by as much as 20% in some cases. The KE model is perhaps the most accurate throughout the range of frequencies, a surprising finding given the results obtained from the *a priori* tests described above.

To evaluate the response of the models to the unsteadiness we can consider the component of the phase-averaged velocity at the driving frequency, which is obtained by minimizing in the least-squares sense the function

$$\langle u\rangle(t) - u_0 - u_1\cos(\omega t + \alpha), \qquad (10)$$

where ω is the driving frequency. u_1^+ is shown in Fig. 9. The KEV2 model appears to be the most accurate in reproducing the response of the flow to the unsteadiness, at least as far as the streamwise velocity is concerned.

In our calculations the mean value of the wall stress is determined by the mean pressure gradient, whereas its oscillating part depends on the amplitude and frequency of the pressure-gradient oscillations. At large driving frequencies, the amplitude tends to the one predicted by laminar theory. At low frequencies the ratio of the turbulent to laminar stress diverges as $\omega^{-1/2}$ (see Tardu *et al.*[2]). The two regimes are separated by range of frequencies in which the amplitude is *lower* than the laminar value, a result that has been observed in several experiments,[2,9,23] and confirmed by the LES (Fig. 10). At high frequencies all the models predict a slightly high value of the amplitude. As the frequency is lowered, the models fail to reproduce the reduction in amplitude observed experimentally and by the LES.

We consider next the Reynolds shear stress, shown

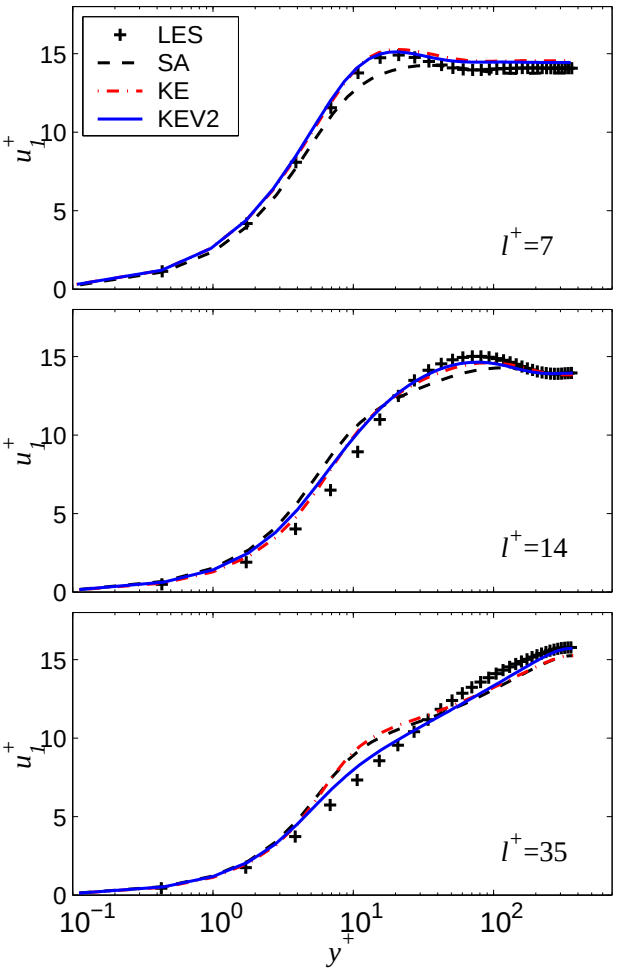

Fig. 9 Streamwise velocity component at the forcing frequency.

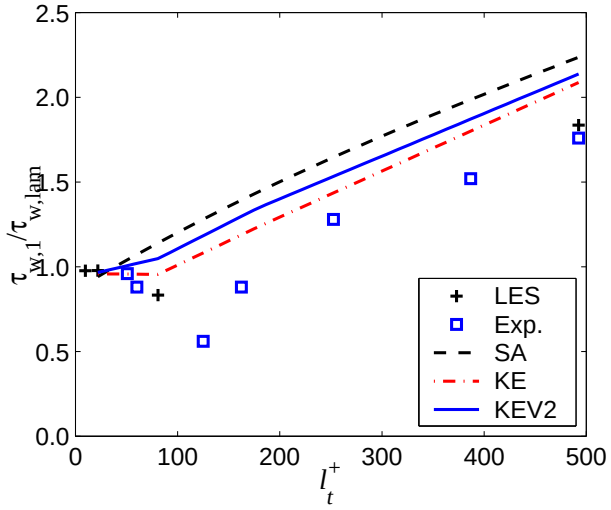

Fig. 10 Amplitude of the component of the wall stress at the driving frequency, normalized with the amplitude of the wall stress in a laminar flow driven at the same frequency.

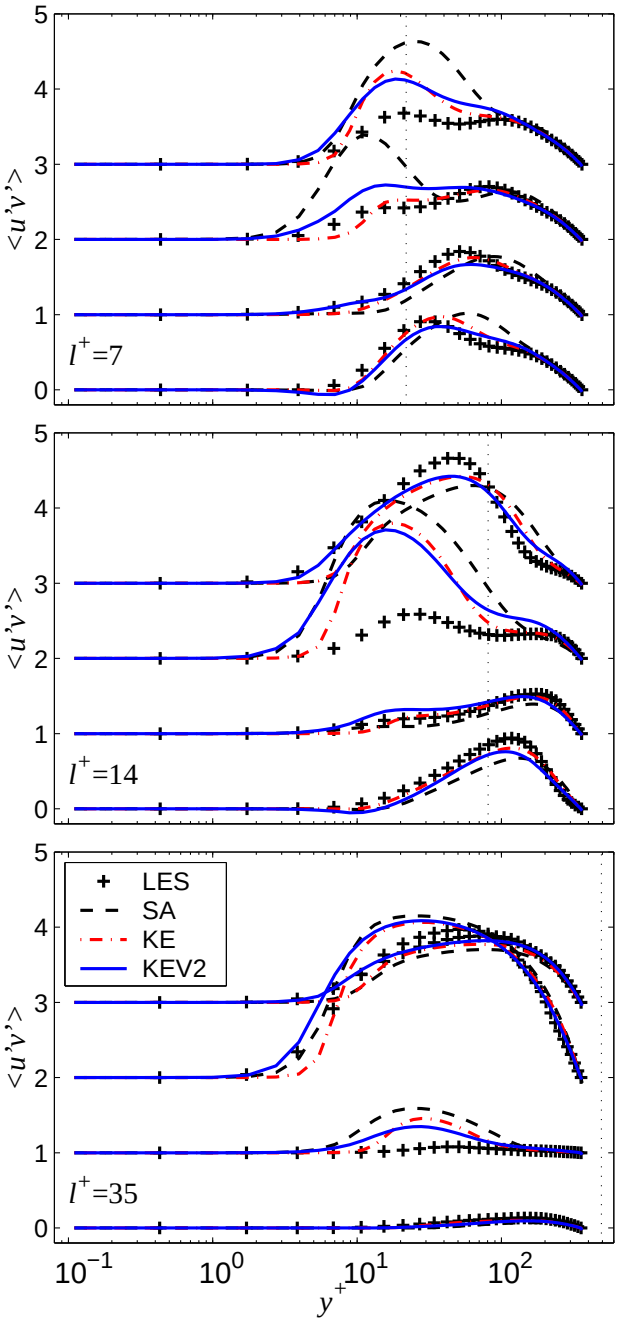

Fig. 11 Profiles of the phase-averaged Reynolds shear stress. Profiles are plotted every $T/4$ and offset in the vertical direction; the bottom plot corresponds to $t/T = 0$. The dotted line corresponds to the turbulent penetration length l_t^+ given by (8).

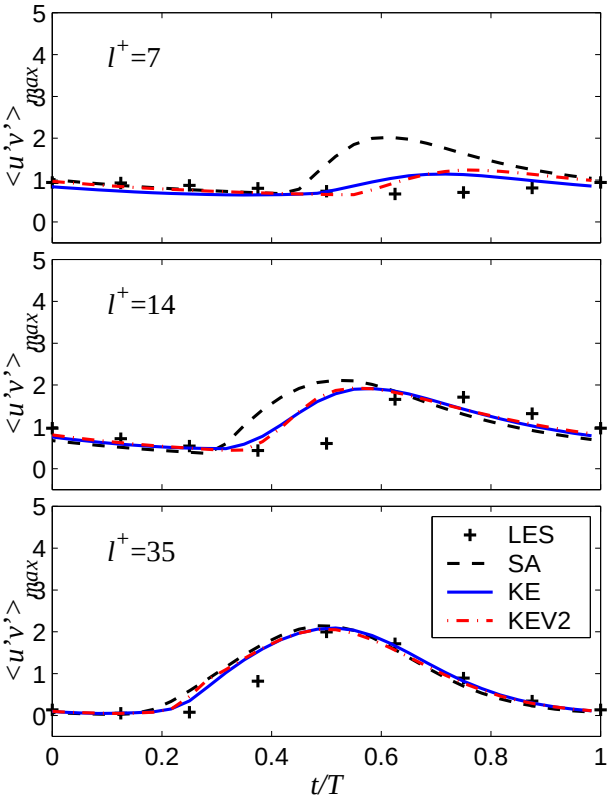

Fig. 12 Time series of the maximum phase-averaged Reynolds shear stress $\langle u'v' \rangle$.

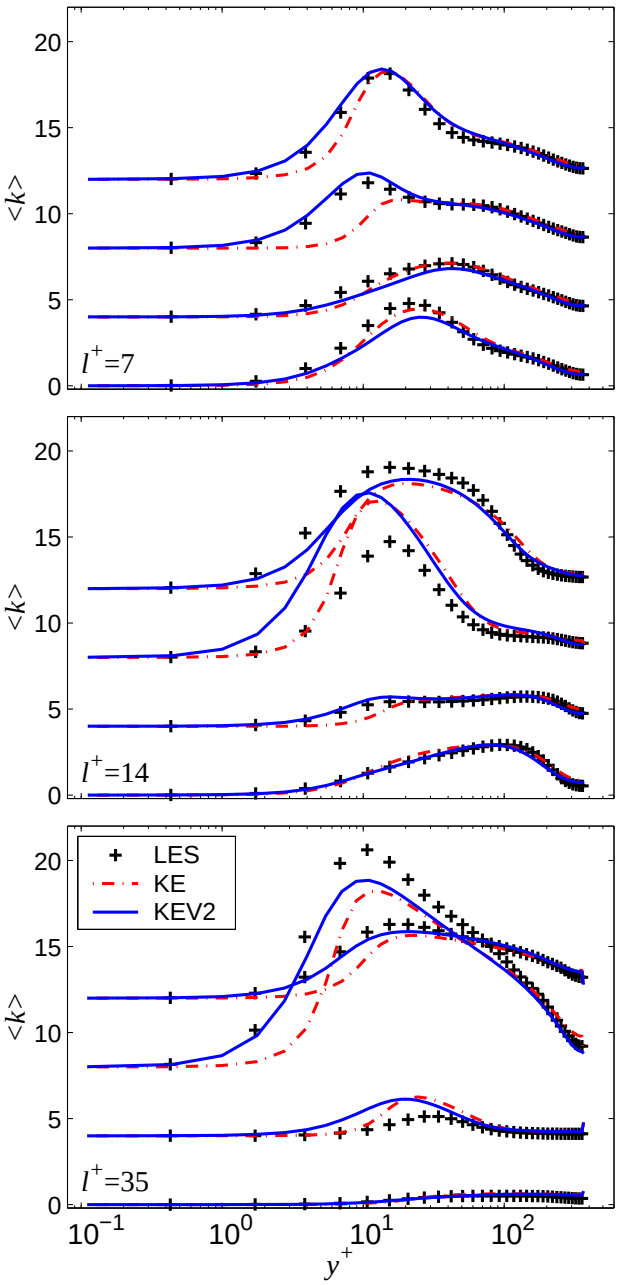

Fig. 13 Profiles of the phase-averaged turbulent kinetic energy k. Profiles are plotted every $T/4$ and offset in the vertical direction; the bottom plot corresponds to $t/T = 0$.

in Fig. 11. At high frequency, the models predict the correct behavior during the acceleration phase, especially outside the region $y^+ = 2l_i^+$. In the region affected by the vorticity waves, on the other hand, the Reynolds-stress increase that is observed in the LES at the beginning of the deceleration phase is overestimated by all models. Also, the increase begins too early. This is also clearly shown in Fig. 12, in which the peak $\langle u'v' \rangle$ is shown. The substantial overestimation of $\langle u'v' \rangle_{max}$ by the KE model that was observed in the *a priori* tests is not present here, indicating that the self-correcting features of the model improve the results. Of the three models tested, KEV2 appears to be the most accurate.

At intermediate frequencies we observe similar trends. The SA model underestimates the stress during the initial phase, and severely overestimate the stress increase coinciding with the onset of deceleration. KE and KEV2 fare better during acceleration, but behave in a manner similar to SA during the deceleration, although with a smaller error. The early beginning of the Reynolds stress increase is at this frequency most notable (Fig. 12). At low frequency a similar conclusions can be drawn: the largest deviation occurs during the last stage of the acceleration phase. As shown before, the flow is essentially laminar during the early accelerating phase, and all the models transition to turbulence early. It should be pointed out that URANS models of this type may have difficulties predicting transition. The SA model, in particular, assumes that the transition point is known, and may not be expected to predict transition accurately.

In the case of KE and KEV2 in addition to $\langle u'v' \rangle$ we can compare the turbulent kinetic energy $\langle k \rangle$ and the rate of dissipation $\langle \varepsilon \rangle$ between the URANS and the LES. In Fig. 13 we show $\langle k \rangle$. At high frequency KEV2 is in good agreement with the LES for the entire cycle, while KE agrees only during the accelerating phase; during the deceleration phase the KE underestimates

the turbulent kinetic energy in the region $y^+ < 2 * l_t^+$. At the intermediate frequency the situation is similar, but the difference between KEV2 and LES is larger, and at $t/T = 1/2$ the peak energy predicted by KE is larger than in the LES. Again, the acceleration phase, and the late deceleration one are reproduced satisfactorily. At the low frequency we observe a similar pattern, although during the deceleration phase the KE and KEV2 models have less energy than the LES. It must be noted that even in the steady case the energy predicted by the KE model is lower in the inner layer than the LES and DNS.

Finally we show the dissipation $\langle\varepsilon\rangle$ in Fig. 14. KEV2 tends to have more realistic trends in the inner layer, but neither model is particularly accurate. In the decoupled part of the outer layer, on the other hand, the agreement is good at all times.

Discussion

In this paper we have considered three RANS models applied to a channel flow driven by an unsteady pressure gradient. Several interesting features have been brought to attention. *A priori* testing shows that KEV2 model has the potential for giving a fairly accurate estimate of the Reynolds stress, provided that the coefficient C_μ is adjusted. On the other hand, it seems difficult to come up with a satisfactory solution to cure the pitfalls of KE, which appear to be structurally related to setting $\nu_t \sim k^2/\varepsilon$.

The *a posteriori* tests show a more benign outcome. Despite large differences in the Reynolds shear stress relative to the LES, the time evolution of the streamwise velocity seems relatively unaffected. The picture is actually quite complex, since we have to consider simultaneously both the effects on the mean (time-averaged) flow and on its oscillating part. Indeed, changes in the oscillating eddy viscosity will affect the mean flow *via* a rectification mechanism; *vice versa*, changes in the mean eddy viscosity will show up in the oscillating velocity component.

We observe the centerline velocity predicted by the URANS models progressively decreasing as the frequency is lowered. Also, the largest deviation of the oscillating components of the flow occur during the deceleration phase, in which the predicted Reynolds shear stress is farther apart from the observed one. The discrepancies between the URANS models and the LES seem to be limited to about 1/3 to 1/4 of the period T. Thus, at high frequencies the errors are short-lived (compared to the diffusive time-scale in the channel flow) while a lower frequencies the errors live longer and can redistribute momentum on a larger area.

As far as the streamwise velocity is concerned, all model considered perform just similarly, and their accuracy may be acceptable. If, on the other hand, information concerning the Reynolds stress is required, as is the case for instance in sediment transport or medical applications, the SA model does not appear to give sufficient accuracy. Between KE and KEV2, overall the latter appears more accurate, although at the extra cost of solving two additional equations, compared with KE.

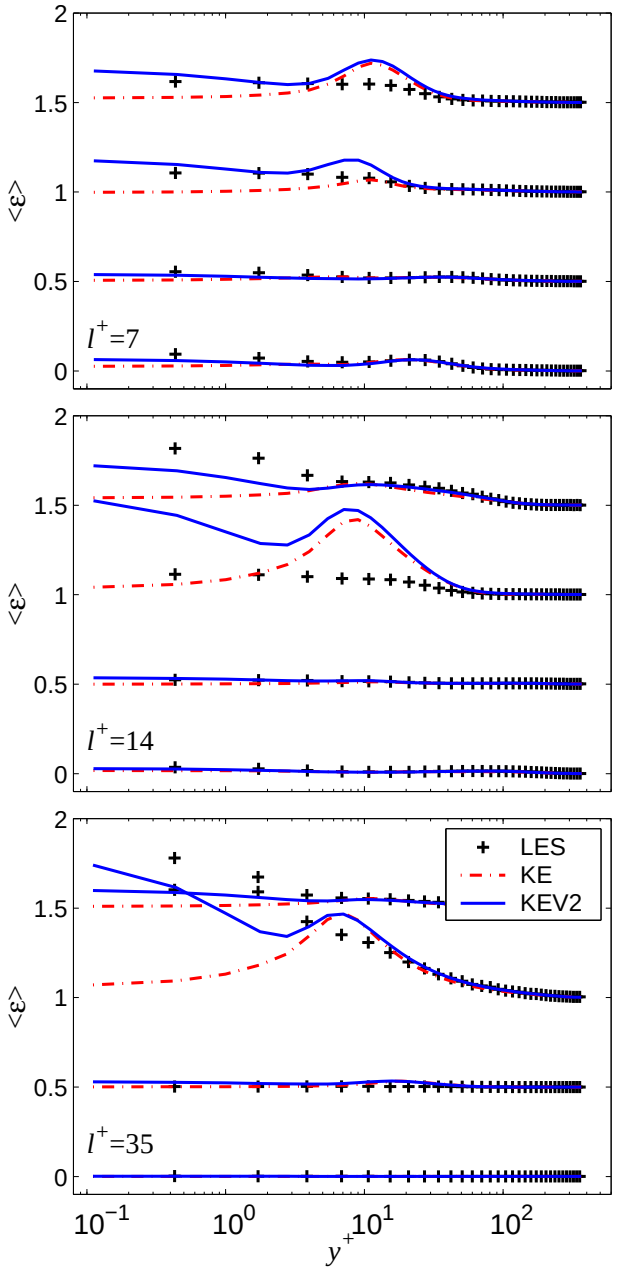

Fig. 14 Profiles of the phase-averaged turbulent kinetic energy dissipation ε. Profiles are plotted every $T/4$ and offset in the vertical direction; the bottom plot corresponds to $t/T = 0$.

Acknowledgment

This work was supported by NSF under grant OCE-99-10883.

References

[1]G. G. Stokes, *Trans. Cambridge Phil. Soc.* **8**, p. 287, (1845).

[2]S. Tardu, G. Binder and R. F. Blackwelder, "Turbulent channel flow with large-amplitude velocity oscillations," *J. Fluid Mech.* **267**, pp. 109–151, (1994).

[3]G. Binder, S. Tardu and P. Vezin, "Cyclic modulation of Reynolds stresses and length scales in pulsed turbulent channel flow," *Proc. Roy. Soc. London, Ser. A* **451**, pp. 121–139, (1995).

[4]S. Tardu and G. Binder, "Wall shear stress modulation in unsteady turbulent channel flow with high imposed frequencies," *Phys. Fluids A* **5**, pp. 2028–2037, (1993).

[5]W. D. Grant and O. S. Madsen, "The continental-shelf bottom boundary layer," *Annu. Rev. Fluid Mech.* **18**, pp. 265–305, (1986).

[6]M. Y. Gündogdu and M. Ö Caprinlioglu, "Present state of art on pulsatile flow theory (Part 1: Laminar and transitional flow regimes)." *JSME Int. J. Series B* **42**, p. 384–397 (1999).

[7]M. Y. Gündogdu and M. Ö Caprinlioglu, "Present state of art on pulsatile flow theory (Part 2: Turbulent flow regime)." *JSME Int. J. Series B* **42**, p. 398–410 (1999).

[8]R. R. Mankbadi and J. T. C. Liu, "Near-wall response in turbulent shear flows subjected to imposed unsteadiness." *J. Fluid Mech.* **238**, pp. 55–71 (1992).

[9]Z.-X. Mao and T. J. Hanratty, "Studies of the wall shear stress in a turbulent pulsating pipe flow." *J. Fluid Mech.* **170**, pp. 545–564 (1986).

[10]J. Reichardt, "Die Grundlagen des Turbulenten Wärmeüberganges." *Arch. Ges. Warmetechnik* **2**, pp. 129–143 (1951).

[11]E. R. Van Driest, "On the turbulent flow near a wall." *J. Aero. Sci.* **23**, pp. 1007–1011 (1956).

[12]U. Piomelli, "High Reynolds number calculations using the dynamic subgrid-scale stress model." *Phys. Fluids A* **5**, pp. 1484–1490 (1993).

[13]M. Germano, U. Piomelli, P. Moin, and W. H. Cabot. "A dynamic subgrid-scale eddy viscosity model." *Phys. Fluids A* **3**, 1760 (1991).

[14]D. K. Lilly."A proposed modification of the Germano subgrid-scale closure method." *Phys. Fluids A* **4**, 633 (1992).

[15]A. Scotti and U. Piomelli, "Numerical simulation of pulsating turbulent channel flow," Submitted to *Phys. Fluids* (2000).

[16]P. R. Spalart and S. R. Allmaras, "A one-equation turbulence model for aerodynamic flows," *La Recherche Aérospatiale* **1**, pp. 5–21, (1994).

[17]C. K. G. Lam and K. A. Bremhorst, "Modified form of the $k-\varepsilon$ model for predicting wall turbulence," *J. Fluids Engng* **103**, pp. 456–460, (1981).

[18]V. C. Patel, W. Rodi and G. Scheuerer, "Turbulence models for near-wall and low Reynolds number flows: A review," *AIAA J.* **23**, pp. 1308–1319, (1985).

[19]P. A. Durbin, "Separated flow computations with the $k-\varepsilon-v^2$ model," *AIAA J.* **3**3, pp. 659–664, (1995).

[20]R. D. Moser, J. Kim, and N. M. Mansour, "Direct numerical simulation of turbulent channel flow up to $Re_\tau = 590$." *Phys. Fluids* **11**, pp. (1999).

[21]P. R. Spalart, W. H. Jou, M. Strelets, and S. R. Allmaras "Comments on the feasibility of LES for wings, and on a hybrid RANS/LES approach." In *Advances in DNS/LES*, edited by C. Liu and Z. Liu, (Greyden Press, Columbus), pp. 137–148 (1997).

[22]Unless otherwise stated, all quantities are normalized using the time-averaged friction velocity u_τ.

[23]D. Ronneberger and C. D. Ahrens. "Wall shear stress caused by signal amplitude perturbations of turbulent boundary layer flow: an experimental investigation." *J. Fluid Mech.* **83**, p. 433 (1977).